■ 681

Error Performance Analysis in Underwater Acoustic Noise with Non-Gaussian Distribution

Nor Shahida Mohd Shah[1], Yasin Yousif Al-Aboosi[2], Musatafa Sami Ahmed*[3]
[1,3]Faculty of Electrical and Electronics Engineering, Universiti Tun Hussein Onn Malaysia (UTHM)
Parit Raja, Batu Pahat, Johor, Malaysia
[2]Faculty of Engineering, University of Mustansiriyah, Baghdad, Iraq
*Corresponding author, e-mail: mustafa_sami87@yahoo.com

Abstract
There is a high demand for underwater communication systems due to the increase in current social underwater activities. The assumption of Gaussian noise allows the use of Traditional communication systems. However, the non-Gaussian nature of underwater acoustic noise (UWAN) results in the poor performance of such systems. This study presents an experimental model for the noise of the acoustic underwater channel in tropical shallow water at Desaru beach on the eastern shore of Johor in Malaysia, on the South China Sea with the use of broadband hydrophones. A probability density function of the noise amplitude distribution is proposed and its parameters defined. Furthermore, an expression of the probability of symbol error for binary signalling is presented for the channel in order to verify the noise effect on the performance of underwater acoustic communication binary signalling systems.

Keywords: Underwater Acoustic Noise, student's t distribution, bit error rate, non-Gaussian signal detection.

1. Introduction

Increased interest in defense applications, off-shore oil industry, and other commercial operations provides a motivation for research in signal processing for the underwater environment. In the underwater environment, acoustics waves are more practical for applications such as navigation, communication, and other wireless applications due to the high attenuation rate of electromagnetic waves. Acoustic propagation is characterized by three major factors: attenuation that increases with signal frequency, time-varying multipath propagation, and low speed of sound (1500 m/s) [1-3]. No two deployment regions within the ocean with have the same depths ranging from tens of meters to a few kilometers with node placement that varies from one network to another [4].

Sources of underwater acoustic noise (UWAN) are manmade (shipping, aircraft over the sea and machinery sounds on the ship) and natural (rain, wind, marine lifeforms and seismic) [5]. As the attenuation of sound in the ocean is frequency dependent, the ocean acts as a low-pass filter for ambient noise. Results ambient noise power spectral density (PSD) is thus described as colored that is the noise has more power at the lower frequencies and less power at the higher frequencies [6]. The ambient noise comes from sources such as turbulence, breaking waves, rain, and distant shipping. While ambient noise is often approximated as Gaussian, in practice it is colored exhibiting a decaying power spectral density (PSD). The rate of decay is at approximately 18 dB/decade [7]. The underwater environment consists also site-specific noise [7]. Site-specific noise, for example, exists for ice cracking in the polar region and acoustic noise due snapping shrimp in warmer waters. Unlike ambient noise, site-specific noise often contains significant non- Gaussian components.

Several papers show that the noise in underwater acoustic channel does not follow the normal distribution. The actually probability density function (PDF) with extended tails shaped characterizes for this type of noise and have an accentuated impulsive behaviour [7-8].

In this paper, an experimental model for the noise of the acoustic underwater channel is developed from the analysis of field data measurements and a pdf is defined. For binary signaling, an expression for the binary error probability is determine for the channel. Additionally, simulations were conducted with experimentally collected noise, in order to define

the performance of binary underwater communication systems. The rest of this paper is organized as follows. Section 2 defines the signal model. Section 3 describes the results of noise model from collected data. The Error Performance Analysis Of binary phase shift keying (BPSK) Signal is explained in section 4. The results and discussion are discussed in Section 5 . Finally, the conclusion of the paper is elaborated in Section 6.

2. Signal Model

Many applications assumed that, the received signal can be defined as follows:

$$x[n] = s[n] + v[n] \tag{1}$$

where $s(n)$ is the M-ary PSK signal of interest and $v(n)$ is the UWAN. The assumptions of Gaussian distribution for UWAN are described in [8]. However, recent work suggested that the UWAN follows t-distribution [9] and stable alpha distribution [10].

The power spectrum density (PSD) of white Gaussian noise is a constant over the complete frequency range, all frequencies range with a magnitude of σ_v^2. For a given time instant, it has shaped probability distribution function pdf $\rho_v(v)$ given by [11]:

$$\rho_v(v) = \frac{1}{\sigma_v \sqrt{2\pi}} e^{-\frac{v^2}{2\sigma_v^2}} \tag{2}$$

where σ_n represent the standard deviation. The delta function on the autocorrelation functions means that adjacent samples are independent with all samples are Gaussian with the same statistical properties. Thus, he observed samples are considered independent identically distributed (i.i.d). Because of the underwater acoustic noise (UWAN) is contain of many individual sources, A precise identification of the distribution is required [5-6]. Some publications have stated that the UWAN does not follow the Gaussian distribution [6, 9, 12, 13]. Instead, it follows probability density function with extended tail shape, reflecting an accentuated impulsive behaviour due to the high incidence of large amplitude noise events. Thus, the distribution of data is appropriately described by the Student's t distribution [14-15].

3. Data Collection and Non-Gaussian Noise Model

Field trials were conducted at Desaru beach (1°35.169'N, 104° 21.027'E) to collect signal samples and investigate the statistical properties of UWAN. The signals were received at a frequency range of 7 Hz –22 KHz by using a broadband hydrophone (Dolphin EAR 100 Series). The measurements were obtained at depths from 1m to 7m from the seafloor, which is at a depth of 8 m. The wind speed was approximately 7 Kn, and the surface temperature was approximately 27C° [14]. Figure 1 shows the time representation of the collected data at depths of 3 meters and 7 meters where the impulsive nature of the noise can be clearly observed.

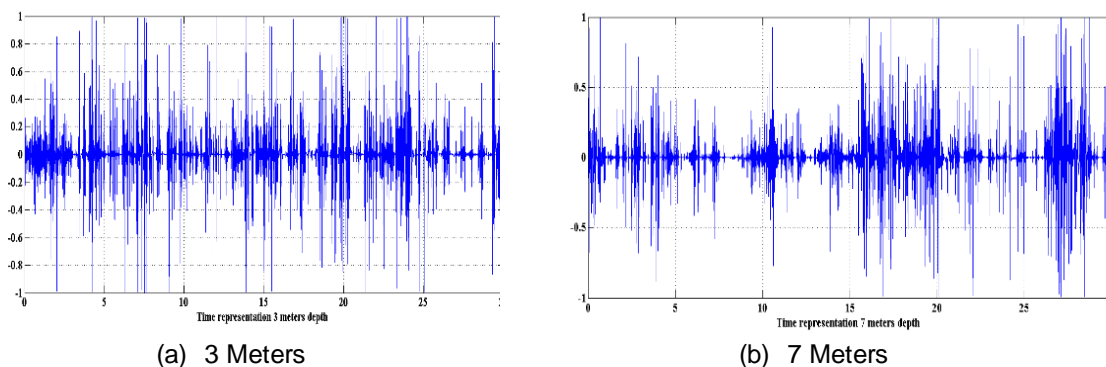| (a) 3 Meters | (b) 7 Meters |

Figure 1. Time Representation of the UWAN at Depths of 3 Meters and 7 Meters.

The distributions obtained from the collected data were compared with the Gaussian distribution and Student's t distribution with the distribution fitting tool in MATLAB. The comparison results clearly show that the amplitude of the UWAN generally follows the Student's t distribution, as shown in Figure 2. Therefore, the UWAN does not validate the assumption of Gaussian distribution. Clearly, the noise amplitude distribution fitted with the Student's t distribution. The Student's t pdf is expressed as [16].

$$\rho_{v,d}(v,d) = \frac{\Gamma\left[(d+1)/2\right]}{\sqrt{\pi d}\,\Gamma(d/2)}\left(1 + \frac{v^2}{d}\right)^{-(d+1)/2} \tag{3}$$

where $\Gamma(\cdot)$ is the gamma function and d is the degree of freedom that controls the dispersion of the distribution. The pdf represented in Equation 3 has a zero mean and a variance equal to $d/(d-2)$ for $d \geq 2$.
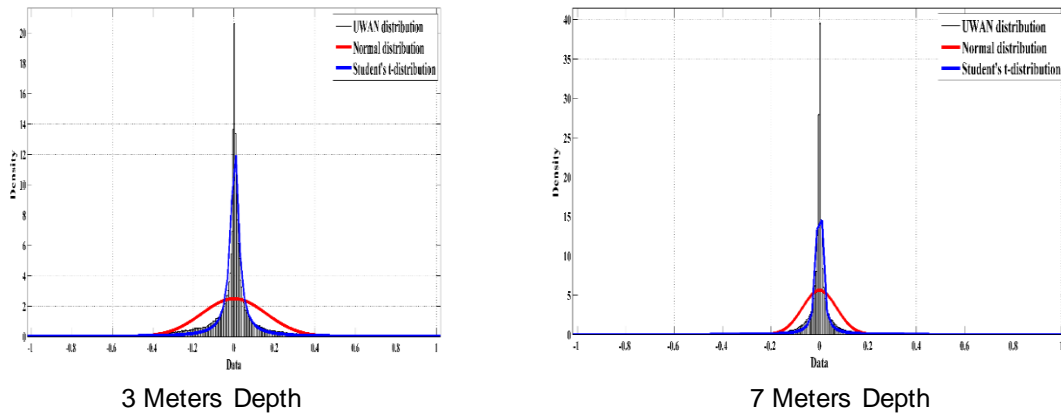

| 3 Meters Depth | 7 Meters Depth |

Figure 2. Comparison of the Amplitude Distribution of the UWAN with the Gaussian Distribution and t-Distribution.

Table 1 indicates the degree of freedom for different depths. For a short period of time, on the order of a few seconds, the UWAN can be assumed to be stationary [17].

Table 1. Degree of Freedom for Different Depth

Depth (m)	Analysis period (Sec)	Degree of freedom (v)
1	1.85	2.94
3	1.26	2.91
5	1.55	2.82
7	1.12	2.8

From the Table above, the average degree of freedom is approximately 3. The analysis of the UWAN shows that its characteristics are not the same as AWGN. The pdf of the UWAN follows a Student's t distribution, in contrast to the assumption of a Gaussian pdf proposed in a previous study [8]. However, to allow modeling a random variable X with variance > 2, it is possible to make the following change of variables:

$$v = \sqrt{\frac{d}{\sigma^2(d-2)}}\,x \tag{4}$$

and consequently, a new scaled pdf function can be written as:

$$f_T(x, d) = \frac{\Gamma\left[(d + 1)/2\right]}{\sigma\sqrt{\pi(d - 2)}\Gamma\left(d/2\right)}\left(1 + \frac{x^2}{\sigma^2(d - 2)}\right)^{-(d+1)/2} \tag{5}$$

For $d = 3$, then the pdf formula is obtained by:

$$f_T(x, 3) = \frac{0.636}{\sigma}\left(1 + \frac{x^2}{\sigma^2}\right)^{-2} \tag{6}$$

and also for $d = 4$, the pdf is:

$$f_T(x, 4) = \frac{0.534}{\sigma}\left(1 + \frac{x^2}{\sigma^2}\right)^{-2.5} \tag{7}$$

4. Error Performance Analysis Of BPSK Signal

From the previously estimated pdf, it is possible to evaluate an expression of the probability of symbol error for binary signaling through the UWAN channel. The system model is as shown in the Figure 3.
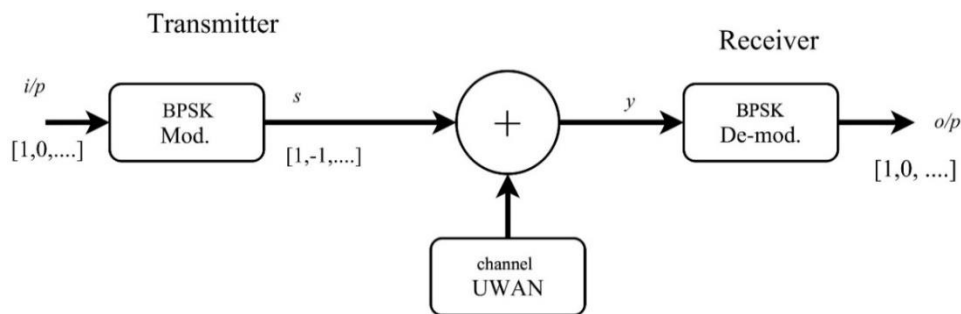

Figure 3. Simplified Block Diagram with BPSK Transmitter-Receiver.

For BPSK signal the amplitudes of the transmitted symbols are given by +A or −A, and then these functions for degree of freedom 3 can be defined as:

$$p(y/s_o) = f(x + A) = \frac{0.636}{\sigma}\left(1 + \frac{(x + A)^2}{\sigma^2}\right)^{-2} \tag{8}$$

$$p(y/s_1) = f(x - A) = \frac{0.636}{\sigma}\left(1 + \frac{(x - A)^2}{\sigma^2}\right)^{-2} \tag{9}$$

Thus, for a binary equiprobable source, the probability of symbol error in the detection of an antipodal signal corrupted by additive noise can be directly calculated by integration of any of the likelihood functions, i.e.

$$P_e = p(s_1)p(e/s_1) + p(s_o)p(e/s_o) \tag{10}$$

if p(s1)=p(s0)=0.5, then:

$$P_e = \int_0^\infty p(e/s_o)\, dx \tag{11}$$

The energy of each bit is given by $E_b = A^2 T_b$, where T_b is the bit interval. In addition, the average power spectral density of the noise can be expressed by $No = \sigma^2/B$, where $B = 1/2T_b$ is the bandwidth occupied by the baseband signal. Without generality loss, assuming that the amplitude of the pulses is unitary, i.e. $A = 1$, then the noise variance σ^2 can be related to the signal-to-noise ratio (SNR) per bit E_b/N_o, according to the following relationship:

$$\sigma^2 = \frac{1}{(2E_b/N_o)} \tag{12}$$

Finally, changing the variables in Equation 8 and applying the result in Equation 11, it follows that the symbol error probability of the binary UWAN channel can be estimated as:

$$P_e = 0.636\sqrt{\frac{2E_b}{N_o}}\int_0^\infty \left[1 + \frac{2E_b}{N_o}(x+1)^2\right]^{-2} dx \tag{13}$$

In same method, for degree of freedom equal 4, the symbol error probability of the binary UWAN channel can be estimated as:

$$P_e = 0.534\sqrt{\frac{2E_b}{N_o}}\int_0^\infty \left[1 + \frac{2E_b}{N_o}\frac{(x+1)^2}{2}\right]^{-2.5} dx \tag{14}$$

The theoretical error performance of the additive white Gaussian noise (AWGN) channel, can be estimated as [18]:

$$P_e = \frac{1}{2}\, erfc\left(\sqrt{\frac{E_b}{N_o}}\right) \tag{15}$$

In the same manner, the symbol error probability of the QPSK modulation and 16-PSK modulation in UWAN channel can be derived.

5. Results and Analysis

The different M-ary PSK modulation techniques (BPSK, QPSK and 16-PSK) are tested in UWAN and compared with the traditional channel (AWGN). Figure 4 shows graphs of the symbol error probability Pe as a function of Eb/No for binary bipolar signaling. The red trace is the estimation for the error probability for the UWAN channel obtained directly from Eq. 13, while black continuous trace shows the theoretical error performance of the additive white Gaussian noise (AWGN) channel. Simulation results, shown as blue continuous trace, are also presented for the UWAN. The Figure 5 shows graphs of the symbol error probability P_e as a function of E_b/N_o for binary bipolar signaling for degree of freedom equal 4.

As can be viewed in Figure 4, the UWAN channel appears to be slightly less prone to errors compared to the AWGN channel, up to a SNR level of approximately 3 dB. After this point, the error probability for the UWAN channel becomes significantly larger in relation to the AWGN channel, and the performance gap enlarges for increasing SNR levels. Although behavior in the UWAN channel at low SNR seems to be counterintuitive, it can be explained due to the shape of the probability density function. The UWAN pdf has wider tails and, consequently, slimmer and taller central body when compared with the normal curve. Thus, for low SNR conditions, i.e., high noise environments, the error probability in (11) corresponds to the area of one entire tail and a considerable portion of the central body half of the pdf. The tail area of the UWAN pdf is larger than the normal but, in compensation, there is section in the

central body where the Gaussian pdf surpasses the UWAN pdf as shown in Figure 6. Since the probability density is higher in the central body, the difference between the areas in this region more than compensates for the area deviation in the tails.
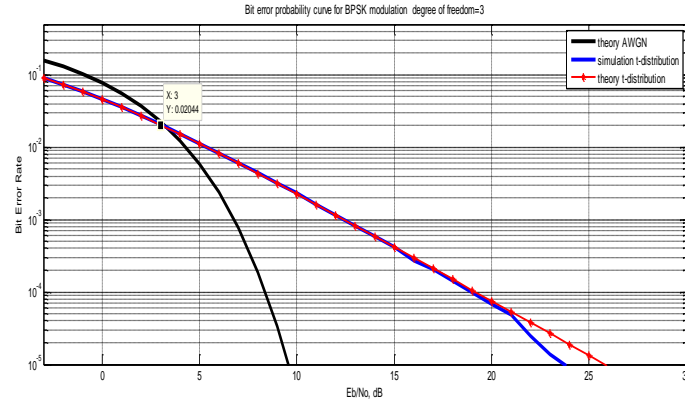

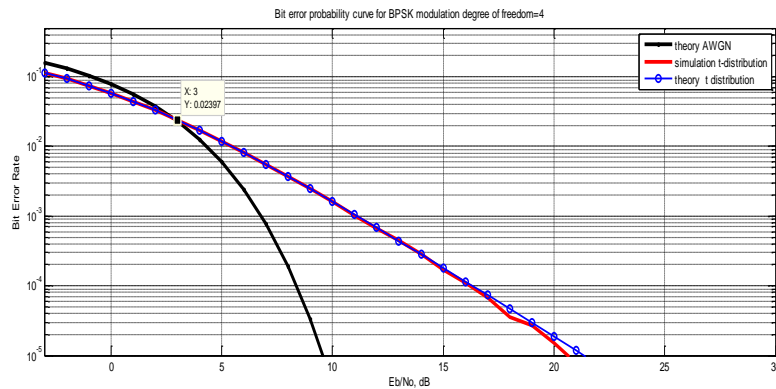Figure 4. symbol error performance for AWGN and UWAN channels with degree of freedom d=3

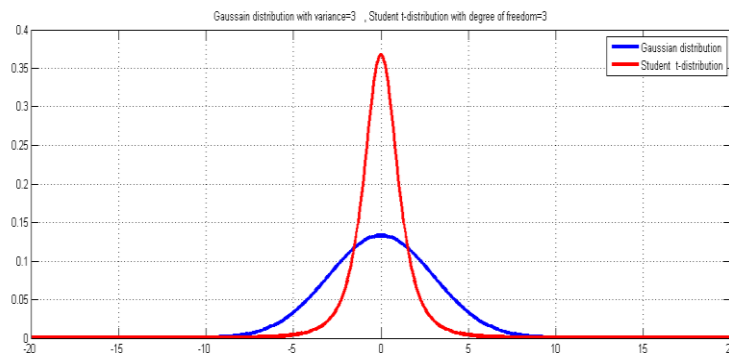Figure 5. Symbol error performance for AWGN and UWAN channels with degree of freedom d=4

Figure 6. Comparison between the amplitude distribution of the underwater acoustic noise and the Gaussian pdf

The symbol error probability is illustrated in Figure 7, where P_e is represented as a function of the E_b/N_o for QPSK signalling for the degree of freedom equal to 3 and 4.

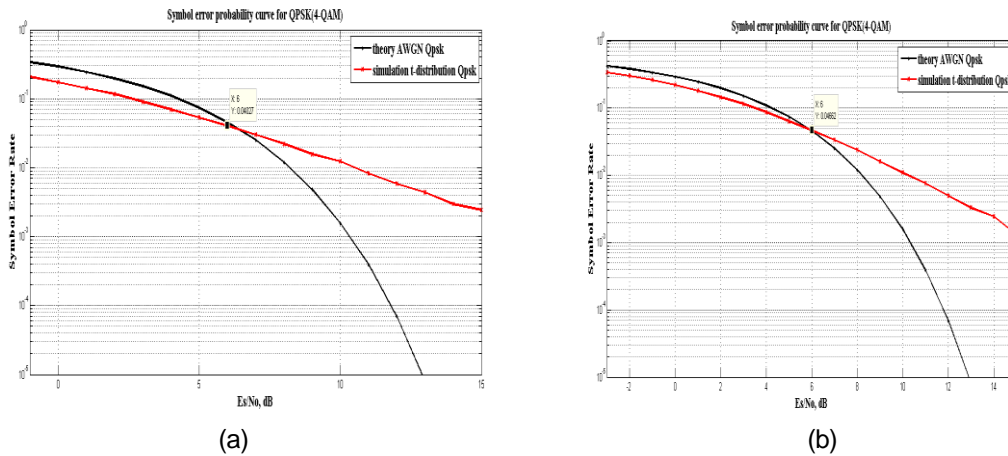(a)   (b)

Figure 7. QPSK symbol error performance for AWGN and UWAN channels with degree of freedom (a)d=3 and (b)=4.

For 16-PSK modulation family, the symbol error probability as a function of E_b/N_o, with 3 and 4 degrees of freedom is presented in figure 8.

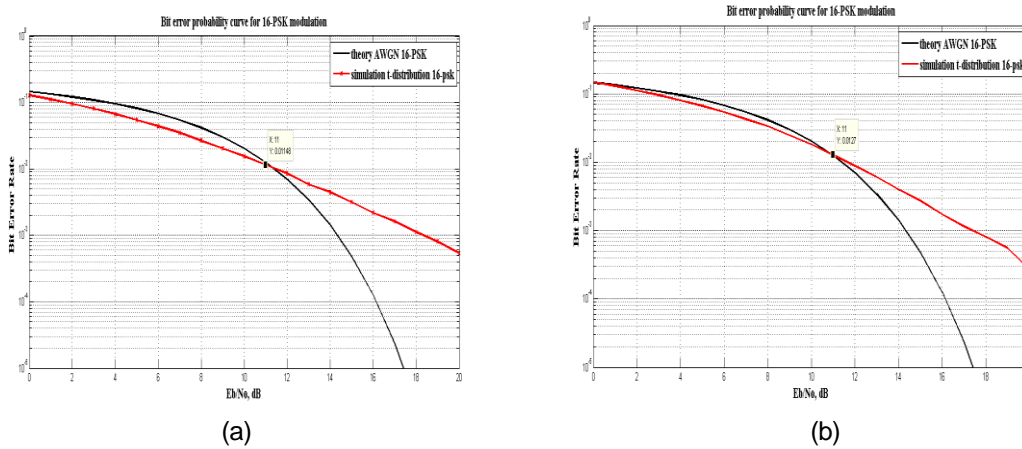(a)   (b)

Figure 8. 16-PSK Symbol Error Performance for AWGN and UWAN Channels with Degree of Freedom (a)d=3 and (b)=4

Table 2 show the SNR critical values which the performance in underwater channel after this values will be worse than the performance in AWGN channel for different modulation techniques and degree of freedom 3 and 4. As shown in Table 2, When the M value for M-ary PSK modulation is increased the critical value for the SNR also increased, on the other hand, the BER for all the M-ary PSK based digital modulation schemes is decreased gradually with increasing values of E_b/N_o.

Table 2. SNR Critical Values for UWAN Channel better than AWGN Channel

Modulation	SNR (dB)	
	d=3	d =4
BPSK	3	3
QPSK	6.5	6.5
16-PSK	11	11

For high SNR environments, as expected, the frequent incidence of impulsive events in the UWAN channel produces severe degradation in the system performance when compared to the AWGN channel. Given the poor performance of the UWAN channel under these conditions, it is recognized that employing some error control coding technique would be essential to mitigate the unwanted effect of the noise and, in this way, contributing to get reliable underwater acoustic communications.

4. Conclusion

Underwater acoustic noise (UWAN) in tropical shallow waters shows an accentuated impulsive behavior and, consequently, does not follow the Gaussian distribution. The analysis of field data measurements has shown that the noise amplitude distribution presents good fitting with the Student's t distribution. Thus, in this article it has been proposed an empirical model for the distribution of the UWAN based on this distribution and the probability density function. The bit error probability could be derived for the uncoded UWAN channel and it was observed that UWAN channel is slightly less prone to errors, compared with the AWGN channel, up to a SNR level of approximately 3 dB, 6.5 dB and 11dB for BPSK, QPSK and 16-PSK modulation techniques respectively. After these points, the error probability for the UWAN channel surpasses the AWGN channel and the difference gradually increasing for high SNR. For high SNR values, the impulsive events produces severe performance is degraded compared with the AWGN channel. Therefore, when the error rates below 10^{-5}, the SNR exceeding 15 dB, 16 dB and 15 dB for BPSK, QPSK, and 16-PSK modulation techniques, respectively.

References

[1]   M. Stojanovic and J. Preisig. Underwater acoustic communication channels: Propagation models and statistical characterization. *Communications Magazine, IEEE.* 2009; 47: 84-89.
[2]   Y. Y. Al_Aboosi, A. Z. Sha'ameri, A. Kanaa. Diurnal Variability Of Underwater Acoustic Noise Characteristics In Shallow Water. *TELKOMNIKA (Telecommunication Computing Electronics and Control),* vol. Under review, 2016.
[3]   Y. Y. Al-Aboosi, M. S. Ahmed, N. S. M. Shah, N. H. H. Khamis. *Study Of Absorption Loss Effects On Acoustic Wave Propagation In Shallow Water Using Different Empirical Models.* 2017; 12: 6474-6478.
[4]   P. King, R. Venkatesan, C. Li. *An improved communications model for underwater sensor networks.* in Global Telecommunications Conference, 2008. IEEE GLOBECOM 2008. IEEE. 2008: 1-6.
[5]   T. Melodia, H. Kulhandjian, L.-C. Kuo, E. Demirors. Advances in underwater acoustic networking," *Mobile Ad Hoc Networking: Cutting Edge Directions.* 2013; 804-852.
[6]   M. Chitre, J. Potter, O. S. Heng. *Underwater acoustic channel characterisation for medium-range shallow water communications.* in OCEANS'04. MTTS/IEEE TECHNO-OCEAN'04. 2004: 40-45.
[7]   G. Burrowes, J. Y. Khan. *Short-range underwater acoustic communication networks*: INTECH Open Access Publisher. 2011.
[8]   R. P. Hodges. Underwater acoustics: Analysis, design and performance of sonar: *John Wiley & Sons.* 2011.
[9]   J. Panaro, F. Lopes, L. M. Barreira, F. E. Souza. *Underwater acoustic noise model for shallow water communications.* in Brazilian Telecommunication Symposium, 2012.
[10]   M. Chitre, J. R. Potter, S.-H. Ong. Optimal and near-optimal signal detection in snapping shrimp dominated ambient noise. *Oceanic Engineering, IEEE Journal of.* 2006; 31: 497-503.
[11]   S. M. Kay. Fundamentals of statistical signal processing, Vol. II: Detection Theory. Signal Processing. Upper Saddle River, NJ: Prentice Hall, 1998.
[12]   S. S. Murugan, V. Natarajan, R. R. Kumar. Estimation of noise model and denoising of wind driven ambient noise in shallow water using the LMS algorithm. *Acoustics Australia.* 2012; 40: 111.
[13]   M. Bouvet, S. C. Schwartz. *Detection in underwater noises modeled as a Gaussian-Gaussian mixture.* in Acoustics, Speech, and Signal Processing, IEEE International Conference on ICASSP'86., 1986; 2795-2798.

[14] A. Z. Sha'ameri, Y. Al-Aboosi, N. H. H. Khamis. *Underwater Acoustic Noise Characteristics of Shallow Water in Tropical Seas.* in Computer and Communication Engineering (ICCCE), 2014 International Conference on. 2014; 80-83.

[15] Y. Y. Al-Aboosi, A. Z. Sha'ameri. Improved underwater signal detection using efficient time−frequency de-noising technique and Pre-whitening filter. *Applied Acoustics*. 2017; 123: 93-106.

[16] M. Ahsanullah, B. G. Kibria, M. Shakil. Normal and Student's T Distributions and Their Applications: Springer, 2014.

[17] R. J. Urick. Ambient noise in the sea. Catholic Univ Of America Washington DC1984.

[18] J. G. Proakis. Digital communications. 1995. McGraw-Hill, New York.